Back Cover: Synthesis and Biological Evaluation of Imidazopyridine-Oxindole Conjugates as Microtubule-Targeting Agents (ChemMedChem 12/2013)

ARTICLE *in* CHEMMEDCHEM · DECEMBER 2013

Impact Factor: 2.97 · DOI: 10.1002/cmdc.201300308 · Source: PubMed

ChemPubSoc Europe

DOI: 10.1002/cmdc.201300308

Synthesis and Biological Evaluation of Imidazopyridine–Oxindole Conjugates as Microtubule-Targeting Agents

Ahmed Kamal,*[a] Vangala Santhosh Reddy,[a] Santosh Karnewar,[b] Sumit S. Chourasiya,[a, c] Anver Basha Shaik,[a] G. Bharath Kumar,[a] Chandan Kishor,[b] M. Kashi Reddy,[a] M. P. Narasimha Rao,[a] Ananthamurthy Nagabhushana,[e, f] Kallaganti V. S. Ramakrishna,[d] Anthony Addlagatta,*[b] and Srigiridhar Kotamraju*[b]

A library of imidazopyridine–oxindole conjugates was synthesised and investigated for anticancer activity against various human cancer cell lines. Some of the tested compounds, such as **10a**, **10e**, **10f**, and **10k**, exhibited promising antiproliferative activity with GI_{50} values ranging from 0.17 to 9.31 μM. Flow cytometric analysis showed that MCF-7 cells treated by these compounds arrested in the G_2/M phase of the cell cycle in a concentration-dependent manner. More particularly, compound **10f** displayed a remarkable inhibitory effect on tubulin polymerisation. All the compounds depolarised mitochondrial membrane potential and caused apoptosis. These results are further supported by the decreased phosphorylation of Akt at Ser473. Studies on embryonic development revealed that the lead compounds **10f** and **10k** caused delay in the development of zebra fish embryos. Docking of compound **10f** with tubulin protein suggested that the imidazo[1,2-*a*]pyridine moiety occupies the colchicine binding site of tubulin.

Introduction

Cancer, the uncontrolled growth of cells, has become a major cause of death throughout the world. Every year more than 20% of the population is affected by cancer, and the mortality rate is increasing annually, making it a major area of focus for researchers.[1,2] Microtubules are dynamic polymers of α and β tubulin present in eukaryotic cells that play a decisive role in several fundamental cellular processes, including cell division, motility, transport, and maintenance of cell shape. In addition microtubules are involved in a host of cell-signalling pathways related to apoptosis. The microtubules are in dynamic equilibrium with tubulin dimers as tubulin is assembled into microtubules, which in turn are disassembled to tubulin.[3–5] Tubulin polymerisation inhibition, therefore results in an increase in the number of cells in metaphase arrest in the cell cycle.[6]

Consequently, microtubules have become an important target for the design of new antimitotic anticancer agents. Drugs that inhibit microtubule polymerisation are effective in the treatment of lung, breast, ovarian, and other cancers. However, occurrence of peripheral neuropathy is a major complication in the development of microtubule depolymerising agents as drugs.[7] Therefore, the discovery of new molecules to overcome neuropathies are required immediately. There has been considerable interest in the discovery and development of small molecules that affect tubulin polymerisation.[2] Colchicines (**1a**), podophyllotoxins (**1b**), and combretastatins, CA-4 (**1c**) are notable examples of compounds that inhibit microtubule assembly by binding to tubulin.[8–10] (Figure 1) CA-4, in particular, is an extensively studied natural *cis*-stilbene that strongly inhibits tubulin polymerisation by binding to the colchicine binding pocket of tubulin.[11–13] However, the success of tubulin polymerisation inhibitors as anticancer agents has stimulated significant interest in the identification of new compounds that may be more potent or more selective in targeted tissues or tumours. Oxindoles are versatile moieties that display diverse biological activities, including anticancer activity.[14–16] Indirubin (**3**), which possess an oxindole moiety as its basic scaffold, is reported as a potent anticancer agent that inhibits cyclin dependent kinase (CDK). Recently has been reported that oxindoles not only inhibited CDK but also tubulin polymerisation by binding at the colchicine binding site.[5,17] More-

[a] *Dr. A. Kamal, V. S. Reddy, S. S. Chourasiya, A. B. Shaik, G. B. Kumar, M. K. Reddy, M. P. Narasimha Rao*
Medicinal Chemistry & Pharmacology Division
Indian Institute of Chemical Technology, Hyderabad 500007 (India)
E-mail: ahmedkamal@iict.res.in

[b] *S. Karnewar, C. Kishor, Dr. A. Addlagatta, Dr. S. Kotamraju*
Centre for Chemical Biology
Indian Institute of Chemical Technology, Hyderabad 500007 (India)
E-mail: anthony@iict.res.in
giridhar@iict.res.in

[c] *S. S. Chourasiya*
Department of Medicinal Chemistry
National Institute of Pharmaceutical Education & Research (NIPER)
Hyderabad 500034 (India)

[d] *K. V. S. Ramakrishna*
Centre for NMR & SC, Indian Institute of Chemical Technology
Hyderabad 500007 (India)

[e] *Dr. A. Nagabhushana*
Centre for Cellular & Molecular Biology, Hyderabad 500007 (India)

[f] *Dr. A. Nagabhushana*
Centre of Excellence in Epigenetics
Indian Institute of Science Education and Research, Pune 411021 (India)

Supporting information for this article is available on the WWW under http://dx.doi.org/10.1002/cmdc.201300308.

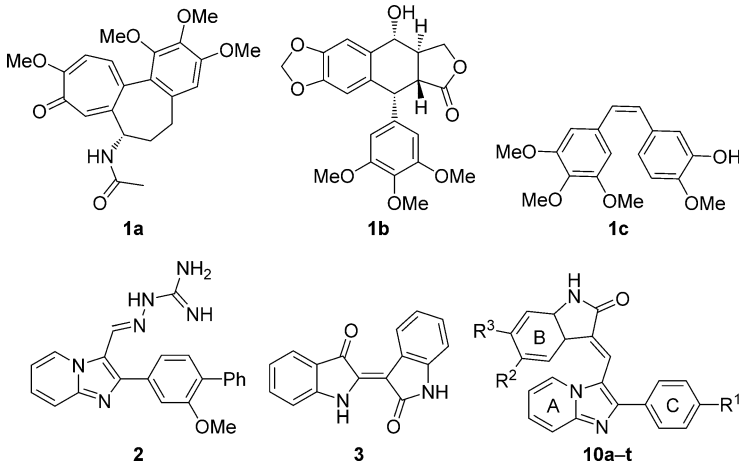

Figure 1. Structures of standard anticancer molecules colchicine (**1a**), podophyllotoxin (**1b**), CA-4 (**1c**), imidazopyridines **2**, indirubin (**3**), and imidazopyridine–oxindole analogues **10a–t**; see Scheme 1 for R^1, R^2, and R^3 groups.

over another class of compounds, namely imidazopyridine (**2**) (Figure 1), possess many biological activities such as antipyretic, anti-inflammatory, antiplatelet aggregation,[18] and anticancer activities.[19] Some of the potent hybrid molecules that have been recently developed as new anticancer agents are obtained by the combination of different pharmacophores.[20,21] The promising biological activity exhibited by these conjugates prompted us to explore some newer conjugates by linking two pharmacophores such as oxindole and imidazopyridine scaffolds to enhance the anticancer activity. In this context we have designed and synthesised imidazopyrimidine–oxindole conjugates (**10a–t**) that were evaluated for their anticancer potential. Interestingly, some of the compounds such as **10a**, **10e**, **10f**, and **10k**, could be considered as potential lead conjugates with impressive antiproliferative activities (GI_{50} 0.17–9.31 μM) against different human cancer cell lines (Table 1). Furthermore, flow cytometric analysis was performed to determine the effect of active congeners in altering the cell-cycle phase distribution in MCF-7 cells. The results of cell cycle and mitotic arrest showed that these compounds affect the G_2/M phase along with the inhibition of tubulin assembly.

Table 1. In vitro cytotoxic effect of conjugates **10a**, **10e**, and**10f** against a panel of 60 human cancer cell lines.

Panel/cell lines	GI_{50} [μM][a]			Panel/cell lines	GI_{50} [μM][a]		
	10a[b]	**10e**[c]	**10f**[d]		**10a**[b]	**10e**[c]	**10f**[d]
Leukaemia				*Ovarian cancer*			
HL-60 (TB)	2.59	1.88	0.34	IGROV1	2.59	3.06	1.09
MOLT-4	4.20	2.89	0.59	OVCAR-3	4.26	1.89	0.28
SR	4.98	2.92	0.29	OVCAR-4	6.21	2.30	1.28
CCRF-CEM	2.57	2.31	0.58	OVCAR-5	4.39	2.21	1.76
RPMI-8226	2.67	2.25	0.92	OVCAR-8	4.90	2.28	1.08
				NCI/ADR-RES	2.01	2.30	0.29
Non-small-cell lung cancer				SK-OV-3	1.95	2.18	1.32
A549/ATCC	3.90	2.14	0.61				
EKVX	3.10	3.08	2.47	*Renal cancer*			
HOP-62	2.70	2.35	1.03	786-0	5.98	2.18	1.04
HOP-92	3.98	1.86	NT[e]	A498	5.87	1.21	0.32
NCI-H226	4.50	2.07	NT[e]	ACHN	4.45	3.25	1.05
NCI-H23	3.77	2.37	0.44	CAKI-1	2.70	2.25	0.66
NCI-H322M	3.68	3.69	1.95	RXF 393	2.75	1.86	0.36
NCI-H460	3.24	2.35	0.39	SN12C	4.91	2.88	1.12
NCI-H522	1.83	2.17	0.18	TK-10	5.05	2.95	1.04
				UO-31	1.95	2.10	0.44
Colon cancer							
COLO 205	2.21	4.03	0.57	*Breast cancer*			
HCC-2998	4.56	2.01	1.04	MCF-7	3.52	2.71	0.38
HCT-116	3.61	2.36	0.43	MDA-MB-231/ATCC	7.29	3.50	1.18
HCT-15	3.60	3.15	0.58	HS 578T	9.31	2.20	1.02
HT29	3.05	2.33	0.32	BT-549	3.97	2.46	NT[e]
KM12	2.55	2.04	0.43	T-47D	4.40	4.35	0.95
SW-620	3.02	3.00	0.36	MDA-MB-468	2.10	2.08	0.25
CNS cancer				*Melanoma*			
SF-268	5.23	2.34	1.25	LOX IMVI	4.34	2.06	0.86
SF-295	NT[e]	1.87	0.38	MALME-3M	3.88	3.80	0.58
SF-539	3.96	2.09	0.88	M14	2.48	3.02	0.54
SNB-19	4.93	3.33	1.43	MDA-MB-435	3.86	1.99	0.17
SNB-75	1.85	2.08	0.39	SK-MEL-2	2.35	2.66	NT[e]
U251	3.97	2.05	0.45	SK-MEL-28	5.53	3.33	1.13
				SK-MEL-5	2.83	2.38	0.41
Prostate cancer				UACC-257	8.96	3.11	1.17
PC-3	3.14	2.43	0.81	UACC-62	3.88	2.58	0.73
DU-145	4.47	2.67	1.12				

[a] Compound concentration required to decrease cell growth to 50% that of untreated cells. Values are single determinations; [b] **10a** (NSC 761116); [c] **10e** (NSC 761121); [d] **10f** (NSC 761130); [e] Not tested.

Results and Discussion

Chemistry

The imidazopyridine–oxindole conjugates **10a–t** were synthesised by employing the Knoevenagel reaction between equimolar mixtures of substituted imidazo[1,2-*a*]pyridine aldehydes (**8a–e**) and oxindoles (**9a–d**). The compound structures were confirmed by means of ^{1}H NMR, ^{13}C NMR, HRMS, and IR spectra. All the compounds were obtained in pure *E* isomeric forms and conformed with those previously reported.[22,23] The key intermediates, imidazo[1,2-

a]pyridine aldehydes (**8a**–**e**) were prepared by means of Vilsmeier–Haack reaction on the corresponding imidazo[1,2-*a*]pyridine (**7a**–**e**) that were in turn obtained by the reaction between 2-aminopyridine and substituted 2-bromo-1-phenylethanones (**4a**–**e**).[24] The sequential steps of these reactions are outlined in Scheme 1.

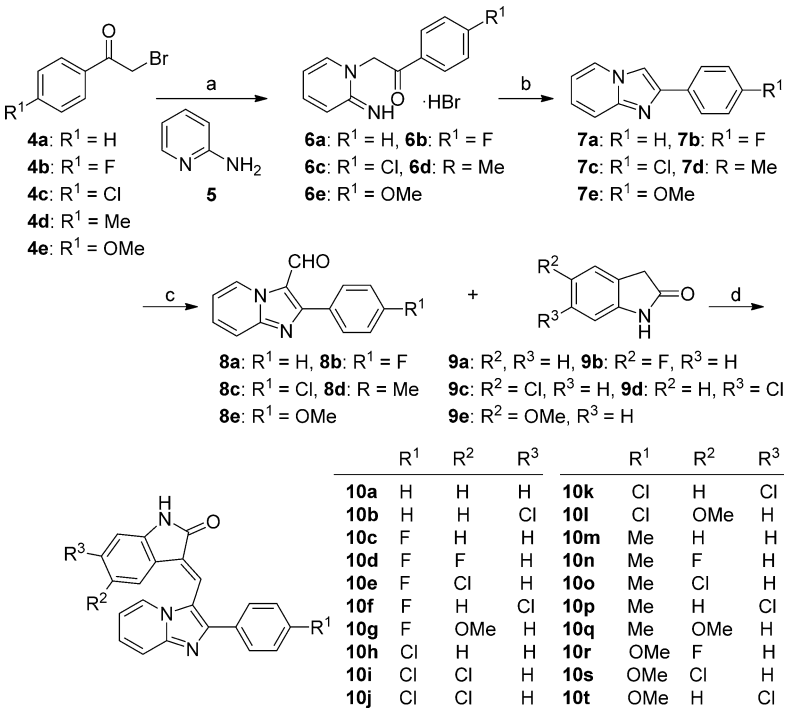

	R^1	R^2	R^3		R^1	R^2	R^3
10a	H	H	H	**10k**	Cl	H	Cl
10b	H	H	Cl	**10l**	Cl	OMe	H
10c	F	H	H	**10m**	Me	H	H
10d	F	F	H	**10n**	Me	F	H
10e	F	Cl	H	**10o**	Me	Cl	H
10f	F	H	Cl	**10p**	Me	H	Cl
10g	F	OMe	H	**10q**	Me	OMe	H
10h	Cl	H	H	**10r**	OMe	F	H
10i	Cl	Cl	H	**10s**	OMe	Cl	H
10j	Cl	Cl	H	**10t**	OMe	H	Cl

Scheme 1. Synthesis of compounds **10a**–**t**. *Reagents and conditions*: a) acetone, reflux, 6–8 h; b) 2 N HCl, reflux, 1 h, 85–92%; c) $POCl_3$, DMF, CH_3Cl_3, 3 h at RT, 10–12 h at reflux, 75–80%; d) substituted oxindoles **9a**–**d**, piperidine, C_2H_5OH, reflux 3–5 h, 50–70%.

Biology

Antiproliferative Activity

Some of the imidazopyridine–oxindole conjugates **10a**–**t** were evaluated for their antiproliferative activity in a panel of 60 human cancer cell lines derived from nine cancer types (breast, non-small-cell lung, colon, CNS, melanoma, ovarian, leukaemia, renal, and prostate cancer cells) by the National Cancer Institute (NCI), Bethesda, MD, USA (see Table 1). For the selected representative compounds **10a**, **10e**, and **10f**, dose–response curves for each cell line were measured at a minimum of five concentrations. Cells were incubated with compounds for a period of 48 h and then cell viability was measured by the sulforhodamine B (SRB) assay. The compounds tested (**10a**, **10e**, and **10f**) showed impressive anticancer activity against the complete panel of 60 cell lines with GI_{50} values ranging from 0.17–9.31 μM. In particular conjugate **10f**, which contains a fluorine substituent at the C4 position of the C ring and a chlorine substituent at the C6 position of the B ring, exhibited significant growth inhibitory activity with GI_{50} values of 0.38 and 0.17 μM against MCF-7 and MDA-MB 435 cell lines, respectively. The conjugate **10k**, which possesses a chlorine atom at the C4 position of the C ring and at the C6 position of the B ring also showed cytotoxicity against MCF-7 (GI_{50} = 0.59 μM) and MDA-MB 435 (GI_{50} = 1.51 μM) cell lines (see Table 2). However, the conjugates **10e** and **10j** contain a chlorine atom at the C5 position of the B ring instead of at the C6 position and showed a decreased cytotoxic effect relative to the conjugates **10f** and **10k** which have the chlorine substitution at the C6 position of the B ring. It is also observed that the absence of a halogen atom on both the B and C rings (**10a**) decreased the antiproliferative activity significantly relative to the halogenated conjugates such as **10e**, **10f**, **10j**, and **10k**. Some conjugates such as **10b**–**d** and **10g**–**t** showed moderate antiproliferative activity as shown in Tables 1 and 2.

Antimitotic effect in MCF-7 cells

In view of the potent antiproliferative activities of these lead conjugates (**10a**, **10e**, **10f**, **10j**, and **10k**) it was of interest to examine cell-cycle alterations caused by these conjugates in MCF-7 breast cancer cells to understand the phase distribution. Thus, cells were treated with these conjugates at concentrations of 3 μM for a period of 24 h. Cells were harvested and analyzed by flow cytometry. It was found that a large proportion of cells treated with conju-

Table 2. Growth inhibition data for compounds **10a**–**t** in selected human breast cancer cell lines.

Compd	GI_{50} [μM][a]		Compd	GI_{50} [μM][a]	
	MCF-7	MDA-MB-231		MCF-7	MDA-MB-231
10a	4.01 ± 0.13	6.35 ± 0.26	**10k**	0.59 ± 0.09	1.51 ± 0.27
10b	3.26 ± 0.30	4.78 ± 0.43	**10l**	4.56 ± 0.12	5.70 ± 0.11
10c	2.17 ± 0.26	2.24 ± 0.27	**10m**	6.23 ± 0.21	7.10 ± 0.08
10d	8.97 ± 0.70	7.61 ± 0.31	**10n**	3.78 ± 0.25	2.67 ± 0.16
10e	2.89 ± 0.37	4.25 ± 0.07	**10o**	4.67 ± 0.36	3.65 ± 0.16
10f	0.43 ± 0.11	0.95 ± 0.31	**10p**	1.35 ± 0.03	1.05 ± 0.21
10g	6.12 ± 0.21	8.21 ± 0.85	**10q**	4.78 ± 0.21	5.21 ± 0.18
10h	4.78 ± 0.17	3.12 ± 0.11	**10r**	5.47 ± 0.65	6.61 ± 0.26
10i	3.98 ± 0.06	4.05 ± 0.02	**10s**	4.56 ± 0.31	3.02 ± 0.21
10j	2.68 ± 0.19	2.91 ± 0.14	**10t**	3.91 ± 0.05	3.10 ± 0.33

[a] Compound concentration required to decrease cell growth to 50% that of untreated cells; values are mean ± SD of three determinations performed in triplicate.

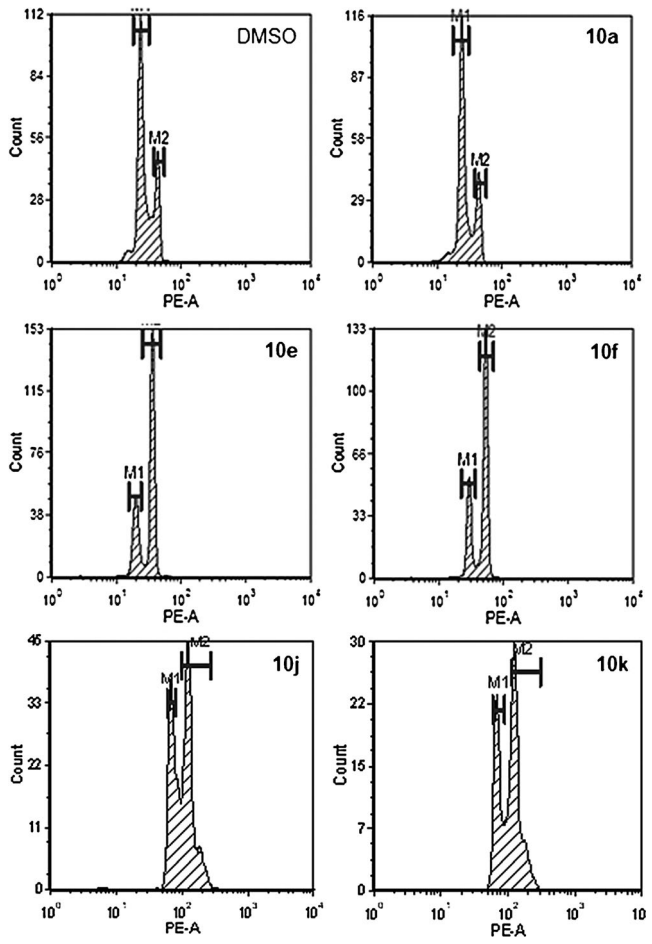

Figure 2. Antimitotic effects of **10a**, **10e**, **10f**, **10j**, and **10k** by FACS analysis. MCF-7 cells were treated with **10a**, **10e**, **10f**, **10j**, and **10k** (3 μM) for 24 h. Untreated cells and DMSO-treated cells served as controls. Cell-cycle analysis was performed with propidium iodide as indicated in the Experimental Section. The cell-cycle phase distribution was determined, and the percentage of cells in each phase was analyzed by FCS express 4 plus.

gates **10e**, **10f**, and **10k** accumulated in the G_2/M phase (68, 63, and 58%, respectively; see Figure 2 and Table 3).

Table 3. Cell cycle phase distribution of MCF-7 cells following treatment with compounds **10a**, **10e**, **10f**, **10j**, and **10k**.

Compd	Phase G_1	S	G_2/M
Control	71.69	8.59	19.72
10a	65.91	13.05	20.99
10e	31.11	5.36	63.53
10f	34.65	6.49	58.86
10j	29.30	19.20	53.71
10k	30.29	6.49	49.62

Inhibition of tubulin polymerisation

To investigate whether the antiproliferative activity of the synthesised congeners was related to an interaction with tubulin, we evaluated their effect on the inhibition of tubulin polymerisation. The imidazopyrimidine–oxindole conjugates (**10a**, **10e**, **10f**, **10j**, and **10k**) were employed at a concentration of 3 μM in tubulin assembly assays. Combretastatin A-4 (**1c**) was used as a positive control. Compounds **10f** and **10k** exhibited potent inhibition of microtubule assembly (72% and 65% inhibition, respectively). Compound **10f** in particular showed tubulin polymerisation inhibition similar to combretastatin A-4 (**1c**). However, compounds **10a**, **10e**, and **10j** also appreciably inhibited tubulin polymerisation, albeit to a lesser extent relative to CA-4. Furthermore, the IC_{50} values of these conjugates was determined and the two leads **10f** and **10k** showed pronounced inhibition of tubulin polymerisation with IC_{50} values of 1.8 μM and 2.4 μM respectively (Table 4). Thereby, these results confirm that compounds **10f** and **10k** are potent inhibitors of tubulin polymerisation.

Table 4. Effect of compounds **10a**, **10e**, **10f**, **10j**, and **10k** on tubulin polymerisation.

Compd	IC_{50} [μM][a]	Inhibition [%][b]
10a	3.8 ± 0.4	47 ± 1.2
10e	2.7 ± 0.2	59 ± 2
10f	1.8 ± 0.01	74 ± 3
10j	3.2 ± 0.5	55 ± 1
10k	2.4 ± 0.2	65 ± 2
CA-4 (**1c**)	1.3 ± 0.1	82 ± 1

[a] Half maximal inhibitory concentration: compound concentration required to inhibit tubulin polymerisation by 50%; data are the mean ± SD of $n = 3$ independent experiments performed in triplicate. [b] Inhibition of tubulin polymerisation at 3 μM (final volume = 10 μL); compounds were pre-incubated with tubulin at a final concentration of 10 μM. Data are the mean ± SD of $n = 3$ independent experiments performed in triplicate.

Effect on mitochondrial membrane depolarisation

Measurement of mitochondrial membrane potential ($\Delta\Psi_m$) serves as a marker to estimate the overall function of mitochondria and during induction of apoptosis, $\Delta\Psi_m$ is depolarised.[25] Therefore, in this study we examined the effect of oxindole conjugates on $\Delta\Psi_m$. MCF-7 cells were treated with compounds **10a**, **10e**, **10f**, **10j**, and **10k** at a 1 μM concentration for 24 h and stained with JC-1 dye. In control cells the dye concentrates in the mitochondrial matrix where it forms red fluorescent aggregates (J-aggregates) because of to the electrochemical potential gradient. In cells treated with compounds which induce apoptosis, the mitochondrial membrane is depolarized thus preventing the accumulation of the JC-1 dye in the mitochondria. Therefore the dye in the monomeric form is dispersed throughout the entire cell leading to a shift from red (J-aggregates) to green fluorescence (JC-1 monomers). Thus, apoptotic cells showing primarily green fluorescence are easily differentiated from healthy cells which show red and green fluorescence. It was observed that these conjugates significantly depolarize the mitochondrial membrane potential (Figure 3) as well as causing significant inhibition of tubulin polymerisation and thereby induce cell death in MCF-7 cells.

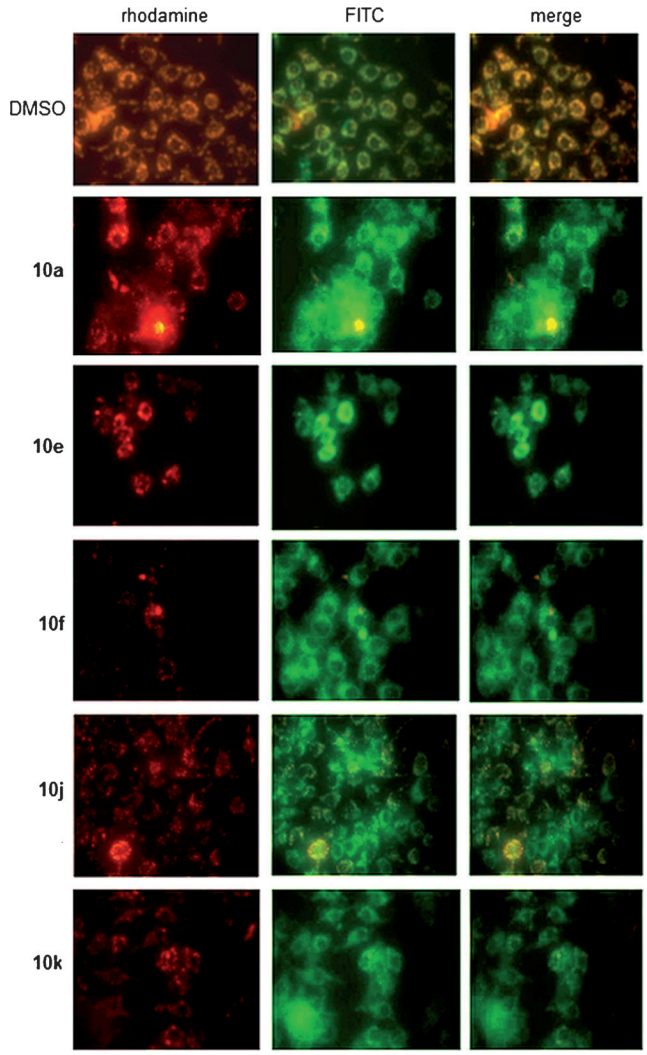

Figure 3. Imidazopyridine–oxindoles cause mitochondrial membrane depolarisation in MCF-7 cells. Cells were treated with **10a**, **10e**, **10f**, **10j**, and **10k** (1 μM) for 24 h, and mitochondrial membrane potential was measured by JC-1 staining as described in the Experimental Section.

Effect on chromatin condensation

Apoptosis is an important, continuous process of destruction of undesirable cells during development or homeostasis in multicellular organisms.[26] During apoptosis, mitochondrial membrane potential is depolarised and chromatin condensation takes place. Hoechst-33258 staining was used to visualise nuclear condensation and it was found that the oxindole conjugates **10a**, **10e**, **10f**, **10j**, and **10k** caused significant nuclear condensation in MCF-7 cells upon treatment at 3 μM concentration for 24 h (Figure 4).

Studies on Akt signaling pathway

It is known that cancer cells possess higher levels of Akt (Ser473), which in turn is responsible for the increased proliferation rates in these cells by inducing downstream cell survival pathways. Interestingly, it was observed that compounds **10e**, **10f**, and **10k**, which caused tubulin depolymerisation, also significantly decreased Akt phosphorylation (Ser473), thereby suggesting that Akt also plays some role in MCF-7 cell death mediated by these conjugates (Figure 5).

Effect on the development of zebra fish embryo

Zebra fish (*Danio rerio*) has emerged as a powerful model system for chemical genetic screening owing to several advantages, especially its external development and optically clear embryos.[27–29] Our results indicate that these conjugates have potent antimitotic activity by destabilising microtubules. To further validate these observations, the effect of these compounds on the development of zebra fish embryos was examined. Zebra fish embryos treated with **10f** and **10k** showed severe delay in development relative to DMSO-treated control embryos. Whereas the control embryos progress through prim5 stage, both the conjugate (**10f** and **10k**) treated embryos were arrested at the 10 somite stage. A similar developmental delay was observed with embryos treated with combretastatin A-4 (**1c**), a known inhibitor of microtubule polymerisation. However, embryos treated with **10a**, **10e**, or **10j** showed little phenotypic abnormalities. These observations suggest that both **10f** and **10k** act as potent antimitotic compounds in zebra fish embryos and could be considered as potential chemotherapeutic leads (Figure 6).

Molecular docking studies

AutoDock version 4.2 was used to dock imidazo[1,2-*a*]pyridine derivatives into the colchicine binding site of β-tubulin.[30,31] Results suggest that the docking position of the imidazo[1,2-*a*]pyridine moiety bind well in the colchicine binding pocket with extensive hydrophobic contacts within the binding pocket of the β-chain (Figure 7). The imidazo[1,2-*a*]pyridine

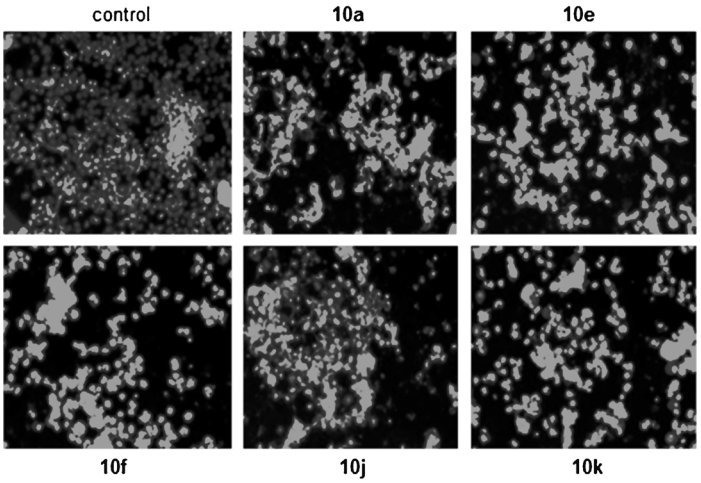

Figure 4. Imidazopyridine–oxindoles cause apoptosis in MCF-7 cells. Cells were treated with **10a**, **10e**, **10f**, **10j**, and **10k** (3 μM) for 24 h, then washed with PBS and incubated with Hoechst-33258 stain (4 μg mL^{-1}) for 20 min to measure nuclear condensation. Fluorescence images were captured with a DAPI filter.

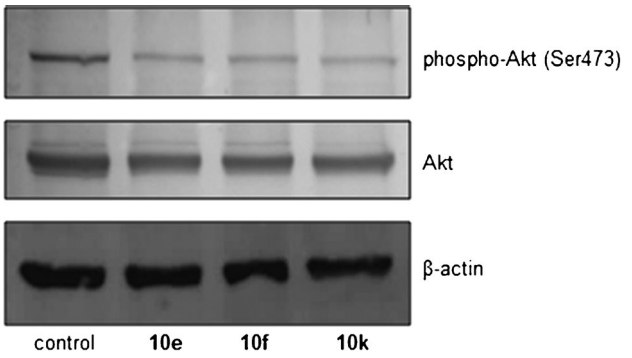

Figure 5. Effect of imidazopyridine–oxindole conjugates on phosphorylation of Akt. MCF-7 cells were treated with **10e**, **10f**, and **10k** (5 μM) for 24 h. Proteins were resolved by SDS-PAGE and immunoblot analysis was performed with Akt and phospho-Akt(Ser473) specific antibodies. The bands were detected by enhanced chemiluminescence as described in the Experimental Section.

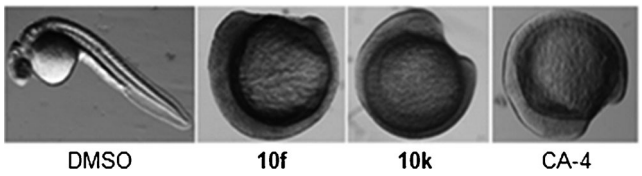

Figure 6. Effect of microtubule inhibitors on the development of zebra fish embryos. Embryos were treated with DMSO (1%), **10f**, **10k** (5 μM) or CA-4 (**1c**) at 5 hpf and imaged at 26 hpf to observe morphology.

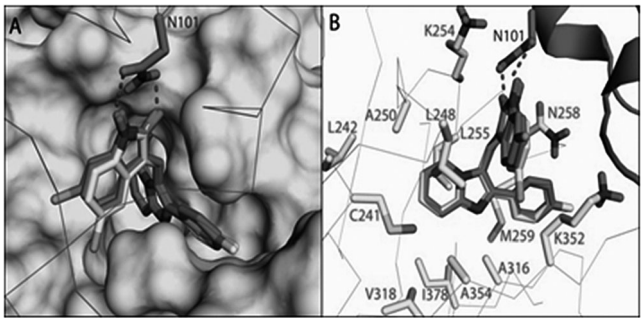

Figure 7. A) Docking pose of **10e** (light sticks) and **10f** (dark sticks). The grey surface represents the β-chain with the blue ribbon indicating the α-chain of tubulin. The imidazo[1,2-*a*]pyridine moiety of compounds is buried in the hydrophobic pocket of the colchicine binding domain. B) Amino acids of α-and β-chain tubulin interacting with compounds **10e** and **10f**. Dashed lines indicate hydrogen bonds.

moiety binds in the pocket where the A ring of colchicine normally binds and amino acids in proximity to this moiety include Cys241, Leu242, Ala250, Leu255, Val318, and Ile378. Whereas the aromatic C ring is sandwiched between Lys352 and Asn258 of the β-chain, the R^1 substituent at the C4 position interacts with the main chain at Asn350. Any larger or hydrophobic groups, such as methyl groups, cannot be accommodated at this position. Compounds that show the highest inhibition against tubulin polymerisation have either no substitution or small atoms such as fluorine or in exceptional cases a chlorine atom (Table 4). The cyclic amide group on indoline (B ring) participates in two hydrogen bonds with Asn101 of the α-chain. The small variation in the substitution at the C5 and C6 positions of B rings shows clear distinction activity. For example, conjugates with a substitution at the C6 position display better inhibition than a conjugate with a substitution at the C5 position. From the modelling it is clear that this ring occupies the interface between the α- and β-chains. The substitution near the C5 position experiences steric clashes with Ly352 of the β-chain, however, the substitution at the C6 position is exposed to solvent and does not have any steric issues and as such they become more favourable to binding. This study further confirms the improved activity of the conjugates **10e** and **10f**.

Conclusions

In conclusion, a library of substituted imidazopyridine–oxindole conjugates **10a**–**t** were synthesised and biologically evaluated for their cytotoxic activity against breast cancer cell lines. Some representative conjugates were evaluated for their antiproliferative potential in the 60 human cancer cell line panel of the NCI. Almost all the synthesised compounds showed excellent to moderate antiproliferative activity, in particular, conjugates **10f** and **10k** showed potent anticancer activity with GI_{50} values as low as 0.6 μM in breast cancer cells. Flow cytometry results demonstrated that these conjugates (**10a**, **10e**, **10f**, **10j**, and **10k**) caused cell-cycle arrest and accumulated cells in the G_2/M phase. These compounds inhibited microtubule assembly as shown by the tubulin polymerisation assay. Interestingly, it was observed that the IC_{50} value of compound **10f** was similar to that of combretastatin A-4 (**1c**), a well-known microtubule assembly disrupter. The docking studies of compounds **10e** and **10f** reveal that the imidazopyridine ring exhibited binding interactions similar to that of the colchicines. SAR results confirm that the conjugates containing a chlorine atom at C6 of the B ring and a halogen atom (F or Cl) at C4 of the C ring showed potent anticancer activity. Based on these results it is evident that compound **10f** is a suitable template for the design of newer tubulin polymerisation inhibitors.

Experimental Section

Biology

Cell-cycle analysis: Breast cancer cells (MCF-7) were incubated for 24 h in the presence or absence of test compounds **10a**, **10e**, **10f**, **10j**, and **10k** (3 μM). Cells were harvested with trypsin EDTA and fixed in ice-cold 70% ethanol at 4 °C for 30 min; ethanol was removed by centrifugation, and cells were stained with 1 mL of DNA staining solution (2 mg of RNase A and 0.2 mg of propidium iodide (PI)) for 30 min.[32] The DNA content of 20000 events were measured by flow cytometry (BD FACS Canto II). Histograms were analyzed using FCS express 4 plus.

Tubulin polymerisation assays: The tubulin polymerisation assay was performed employing a fluorescence-based tubulin polymerisation assay kit (Cytoskeleton, Inc.) according to the manufacturer's protocol.[33,34] The reaction mixture contained, 2 mg mL^{-1} bovine

brain tubulin, 10 μM fluorescent reporter, and 1 mM GTP in the presence or absence of test compounds in PEM buffer (80 mM PIPES, 0.5 mM EGTA, 2 mM MgCl2, pH 6.9) at 37 °C in a final volume of 10 μL. Fluorescence readings were recorded on a Tecan multimode reader at λ 360/420 nm (excitation/emission) every 2 min for up to 3 h. Combretastatin A-4 **(1c)** was used as positive control under similar conditions. To evaluate the IC_{50} values of the compounds against tubulin assembly, the compounds **10a**, **10e**, **10f**, **10j**, and **10k** were incubated at various concentrations (1–5 μM) with tubulin.

Analysis of mitochondrial membrane potential: MCF-7 cells were incubated for a period of 24 h in the presence or absence of test compounds **10a**, **10e**, **10f**, **10j**, and **10k** (1 μM). At the end of treatment, the medium was aspirated, cells were washed with medium without FBS, and JC-1 stain (Sigma cat. no. CS0390) was added to the cells for 20 min at 37 °C under humidified atmosphere. Cells were washed again with medium. The cells were covered with medium and observed under a fluorescence microscope equipped with rhodamine and FITC filters.[25]

Hoechst-33258 staining: MCF-7 cells were incubated for a period of 24 h in the presence or absence of test compounds **10a**, **10e**, **10f**, **10j** and **10k** (3 μM). At the end of treatment, the medium was aspirated, cells were washed with medium without FBS, and Hoechst-33258 stain (Invitrogen cat. no. H3570) was added to the cells for 20 min at 37 °C under humidified atmosphere. Cells were washed again with medium. The cells were covered with medium and observed under a fluorescence microscope equipped with DAPI filter.[26]

Western blot analysis: After the treatment of MCF-7 cells with compounds **10e**, **10f** and **10k** at 3 μM, cells were washed with ice-cold phosphate-buffered saline (PBS) and homogenised in 100 μL of radioimmunoprecipitation assay (RIPA) buffer (20 mM Tris·HCl, pH 7.4, 2.5 mM EDTA, 1% Triton X-100, 1% sodium deoxycholate, 1% SDS, 100 mM NaCl, 100 mM NaF) containing 1 mM sodium orthovanadate and a mixture of protease inhibitors.[35] The homogenate was centrifuged at 750 *g* for 10 min at 4 °C to pellet out the nuclei. The remaining supernatant was centrifuged for 30 min at 12000 *g*. Proteins were resolved on SDS-PAGE and blotted onto nitrocellulose membranes. Membranes were probed with AKT and phospho-AKT (Ser473) procured from Millipore. The detection was carried out with HRP-labelled rabbit anti-mouse IgG (Amersham) using an enhanced chemiluminescence detection system (ECL Advanced Kit, GE Health care).

Zebra fish maintenance and screening: Wild-type zebra fish (*Danio rerio*) were raised and maintained at 28.5 °C with 14/10 h light–dark cycle. Two or three pairs of zebra fish were synchronously mated and embryos were pooled. The embryos were dechorionated and 3–4 embryos were dispensed in 200 μL of E3 embryo medium (5 mM NaCl, 0.17 mM KCl, 0.44 mM $CaCl_2$, 0.68 mM $MgCl_2$) into each well of a 96-well plate. The embryos were treated with compounds **10a**, **10e**, **10f**, **10j**, **10k**, and combretastatin A-4 (**1c**) (5, 10, and 25 μM) and DMSO (1%) at 5 h post-fertilisation (hpf) and incubated at 28.5 °C. Approximately 50 embryos were screened for each compound in biological replicates. They were observed after 28 hpf with a Leica stereomicroscope. Only those compounds that resulted in similar phenotypic defects in most of the embryos were considered active.

Docking studies

Molecular docking simulations were performed using AutoDock 4.2 and the atomic coordinates of β-tubulin as the target (PDB code 3E22). After removing the ligand and solvent molecules, hydrogen atoms and Kollman charges were added to each protein atom. Coordinates for each compound were obtained from Chemdraw11 followed by MM2 energy minimisation. Docking was carried out by AutoDock 4.2 in the colchicine binding pocket.[30,31] Grid map in AutoDock was used to define the interaction of protein and ligand in the binding pocket. The grid map was used with 60 points in each *x*, *y*, and *z* direction, equally spaced at 0.375 Å. Docking was performed using the Lamarckian genetic algorithm.[36] Each docking experiment was performed 100 times, yielding 100 docked conformations. Parameters used for the docking were as follows: population size of 150; random starting position and conformation; maximal mutation of 2 Å translation and 50 degrees rotation; elitism of 1; mutation rate of 0.02 and crossover rate of 0.8; and local search rate of 0.06. Simulations were performed with a maximum of 1.5 million energy evaluations and a maximum of 50000 generations. Final docked conformations were clustered using a tolerance of 1 Å root mean square deviation (RMSD). The best model was chosen based on the most favourable stabilisation energy.

Chemistry

General: All chemicals and reagents were obtained from Lancaster (Alfa Aesar, Johnson Matthey Company, Ward Hill, MA, USA), Sigma–Aldrich (St. Louis, MO, USA), and Spectrochem Pvt. Ltd. (Mumbai, India) and were used without further purification. Reactions were monitored by TLC performed on silica gel coated glass plates containing 60 GF254 with visualisation achieved by UV light or iodine indicator. Column chromatography was performed with Merck 60–120 mesh silica gel. ^{1}H and ^{13}C NMR spectra were recorded on Bruker UXNMR/XWIN-NMR (300 MHz) or Inova Varian VXR Unity (500 MHz) instruments. Chemical shifts (δ) are reported in ppm downfield from an internal TMS standard. ESI mass spectra were recorded on a Micro mass Quattro LC using ESI+ software with a capillary voltage of 3.98 kV and an ESI mode positive ion trap detector. High-resolution mass spectra were recorded on a QSTAR XL Hybrid MS–MS mass spectrometer. Melting points were determined with an Electro thermal melting point apparatus, and are uncorrected. ^{1}H NMR, ^{13}C NMR, and HRMS spectra of final compounds **10a**–**t** are provided in the Supporting Information.

2-Phenylimidazo[1,2-*a*]pyridine (7a): 2-Aminopyridine **5** (1 g, 10 mmol) was dissolved in acetone (100 mL) and treated with **4a** (2.1 g, 10 mmol). The reaction mixture was heated at reflux for 4–5 h, and the resulting salt (**6a**) was collected by filtration, washed with acetone, and then dissolved in 3 N HCl (200 mL) and heated at reflux for 1 h. Before complete cooling, the solution was cautiously basified by dropwise addition of 15% aq NH_4OH to pH 8. The resulting base was collected by filtration and crystallised from EtOH to afford compound **7a** as a white solid (1.75 g, 85% yield); mp: 144–146 °C; ^{1}H NMR (300 MHz, $CDCl_3$): δ = 6.70 (t, J = 6.7 Hz, 1H), 7.10 (dt, J = 6.7, 1.5 Hz, 1H), 7.25 (dt, J = 6.7, 1.5 Hz, 1H), 7.37 (t, J = 7.5 Hz, 2H), 7.57 (d, J = 9.0 Hz, 1H), 7.79 (s, 1H), 7.89 (d, J = 7.5 Hz, 2H), 8.05 ppm (d, J = 6.7 Hz, 1H); MS (ESI): *m/z* 195 $[M+H]^+$.

2-(4-Chlorophenyl)imidazo[1,2-*a*]pyridine (7c): Compound **7c** was prepared according to the method described for compound **7a**, employing 2-Bromo-1-(4-chlorophenyl)ethanone **4c** (2.46 g, 10 mmol) and 2-aminopyridine **5** (1 g, 10 mmol) to obtain the pure

product **7c** as a white solid (2.6 g, 89% yield); mp: 171–173 °C; ^{1}H NMR (300 MHz, $CDCl_3$): δ = 6.77 (t, J = 6.6 Hz, 1H), 7.07–7.21 (m, 3H), 7.62 (d, J = 9.1 Hz, 1H), 7.79 (s, 1H), 7.87–7.96 (m, 2H), 8.10 ppm (d, J = 6.8 Hz, 1H); MS (ESI): m/z 229 $[M+H]^+$.

2-*para*-Tolylimidazo[1,2-*a*]pyridine (7d): Compound **7d** was prepared according to the method described for compound **7a**, employing 2-bromo-1-p-tolylethanone **4d** (2.6 g, 10 mmol) and 2-aminopyridine **5** (1 g, 10 mmol) to obtain the pure product **7d** as a white solid (2 g, 91% yield); mp: 165–168 °C; ^{1}H NMR (300 MHz, $CDCl_3$): δ = 2.38 (s, 3H), 6.78 (dt, J = 6.7 Hz, J = 1.1 Hz, 1H), 7.18 (dt, J = 6.7, 1.2 Hz, 1H), 7.24 (s, 1H), 7.66 (d, J = 9.1 Hz, 1H), 7.82–7.87 (m, 4H), 8.11 ppm (td, J = 6.7 Hz, J = 1.1 Hz, 1H); MS (ESI): m/z 209 $[M+H]^+$.

2-Phenylimidazo[1,2-*a*]pyridine-3-carbaldehyde (8a): The Vilsmeier reagent was prepared at 0–5 °C by dropping $POCl_3$ (2.5 mL, 10.5 mmol) into a stirred solution of DMF (2 mL, 10 mmol) in $CHCl_3$ (10 mL). The 2-phenylimidazo[1,2-*a*]pyridine **7a** (500 mg, 2.6 mmol) in chloroform (20 mL) was added to Vilsmeier reagent whilst maintaining stirring and cooling. The reaction mixture was kept at RT for 3 h and at reflux for 10–12 h (according to a TLC test). Chloroform was removed under reduced pressure and the resulting oily liquid was poured onto ice. The aldehyde **8a** was collected by filtration and crystallised from EtOH (5 mL) to obtain the pure product **8a** as a white solid (418 mg, 73% yield); mp: 155–158 °C; ^{1}H NMR (300 MHz, $CDCl_3$): δ = 7.14 (t, J = 6.8 Hz, 1H), 7.50–7.62 (m, 4H), 7.81–7.86 (m, 3H), 9.68 (d, J = 6.7 Hz, 1H), 10.08 ppm (s, 1H); MS (ESI): m/z 223 $[M+H]^+$.

2-(4-Chlorophenyl)imidazo[1,2-*a*]pyridine-3-carbaldehyde (8c): Compound **8c** was prepared according to the method described for compound **8a**, employing 2-(4-chlorophenyl)imidazo[1,2-*a*]pyridine **7c** (500 mg, 2.19 mmol) to obtain the pure product **8c** as a white solid (393 mg, 70% yield); mp: 151–153 °C; ^{1}H NMR (300 MHz, $CDCl_3$): δ = 7.16 (t, J = 6.9 Hz, 1H), 7.52 (d, J = 8.5 Hz, 2H), 7.61 (t, J = 6.9 Hz, 1H), 7.75–7.85 (m, 3H), 9.66 (d, J = 6.9 Hz, 1H), 10.05 ppm (s, 1H); MS (ESI): m/z 257 $[M+H]^+$.

2-*para*-Tolylimidazo[1,2-*a*]pyridine-3-carbaldehyde (8d): Compound **8c** was prepared according to the method described for compound **8a**, employing 2-(4-chlorophenyl)imidazo[1,2-*a*]pyridine **7d** (500 mg, 2.4 mmol) to obtain the pure product **8d** as a white solid, yield (442 mg, 78% yield); mp: 169–171 °C; ^{1}H NMR (300 MHz, $CDCl_3$): δ = 2.45 (s, 3H), 7.12 (dt, J = 6.9, 1.2 Hz, 1H), 7.35 (d, J = 7.9 Hz, 2H), 7.58 (dt, J = 6.8 Hz, J = 1.2 Hz, 1H), 7.74 (d, J = 8.1 Hz, 2H), 7.80 (td, J = 9.0 Hz, J = 1.1 Hz, 1H), 9.66 (td, J = 6.9, 1.1 Hz, 1H), 10.06 ppm (s, 1H); MS (ESI): m/z 237 $[M+H]^+$.

(*E*)-3-((2-Phenylimidazo[1,2-*a*]pyridin-3-yl)methylene)indolin-2-one (10a): An appropriate mixture of 2-phenylimidazo[1,2-*a*]pyridine-3-carbaldehyde **8a** (200 mg 0.9 mmol) and indolin-2-one **9a** (120 mg, 0.9 mmol) was dissolved in EtOH (10 mL) and piperidine (2–3 drops) was added. The reaction mixture was held at reflux for 3–5 h (according to a TLC test) and the precipitate formed on cooling was collected by filtration and crystallisation with EtOH to obtain the pure product **10a** as a yellow solid (200 mg, 66%); mp: 288–299 °C; IR (KBr) $\tilde{\nu}$ = 3405, 3075, 1712, 745 cm^{-1}; ^{1}H NMR (300 MHz, $CDCl_3$): δ = 6.37 (d, J = 7.9 Hz, 1H), 6.83 (t, J = 7.9 Hz, 1H), 7.02 (d, J = 7.9 Hz, 1H), 7.32 (t, J = 7.9 Hz, 1H), 7.48 (t, J = 8.9 Hz, 1H), 7.52–7.60 (m, 3H), 7.73 (d, J = 6.9 Hz, 2H), 7.79 (s, 1H), 8.03 (t, J = 8.9 Hz, 1H), 8.10 (d, J = 8.9 Hz, 1H), 8.30 ppm (d, J = 8.9 Hz, 1H), 9.26 (s, 1H); ^{13}C NMR (300 MHz, $CDCl_3$ + 1 drop [D]TFA): δ = 169.6, 141.8, 140.5, 137.5, 134.2, 132.4, 131.8, 129.8, 128.9, 128.3, 126.7, 125.4, 124.9, 123.4, 121.4, 119.4, 118.1, 115.8, 114.0, 111.4 ppm; MS (ESI): 338 $[M+H]^+$; HRMS (ESI) calcd for $C_{22}H_{16}N_3O$ $[M+H]^+$ 338.1287; found: 338.1286.

(*E*)-6-Chloro-3-((2-phenylimidazo[1,2-*a*]pyridin-3-yl)methylene)indolin-2-one (10b): Compound **10b** was prepared according to the method described for compound **10a**, employing 2-phenylimidazo[1,2-*a*]pyridine-3-carbaldehyde **8a** (200 mg, 0.9 mmol) and 6-chloroindolin-2-one **9d** (150 mg, 0.9 mmol) to obtain the pure product **10b** as a yellow solid (197 mg, 59%); mp: 309–310 °C; IR (KBr) $\tilde{\nu}$ = 3408, 3004, 1712, 754 cm^{-1}; ^{1}H NMR (300 MHz, $CDCl_3$): δ = 6.32 (d, J = 7.6 Hz, 1H), 6.78 (dd, J = 2.0 Hz, J = 7.6 Hz, 1H), 7.10 (s, 1H), 7.44–7.48 (m, 2H), 7.55–7.63 (m, 2H), 7.68 (d, J = 7.1 Hz, 2H), 7.80 (s, 1H), 8.00 (t, J = 8.8 Hz, 1H), 8.04 (d, J = 8.8 Hz, 1H), 8.19 (d, J = 8.8 Hz, 1H), 9.24 ppm (s,1H); ^{13}C NMR (300 MHz, $CDCl_3$ + 1 drop [D]TFA): δ = 166.7, 143.0, 141.9, 140.7, 137.8, 133.7, 131.7, 129.6, 129.0, 128.4, 126.3, 125.6, 123.0, 122.1, 120.5, 117.9, 115.3, 114.3, 113.1, 111.6 ppm; MS(ESI): 372 $[M+H]^+$; HRMS (ESI) calcd for $C_{22}H_{15}N_3OCl$ $[M+H]^+$ 372.09; found: 372.09.

(*E*)-3-((2-(4-Fluorophenyl)imidazo[1,2-*a*]pyridin-3-yl)methylene) indolin-2-one (10c): Compound **10c** was prepared according to the method described for compound **10a**, employing 2-(4-fluorophenyl)imidazo[1,2-*a*]pyridine-3-carbaldehyde **8b** (200 mg, 0.83 mmol) and indolin-2-one **9a** (111 mg, 0.83 mmol) to obtain the pure product **10c** as a yellow solid (204 mg, 69%); mp: 247–248 °C; IR (KBr) $\tilde{\nu}$ = 3430, 3188, 1691, 757 cm^{-1}; ^{1}H NMR (300 MHz, $CDCl_3$): δ = 6.35 (d, J = 7.8 Hz, 1H), 6.82 (t, J = 7.8 Hz, 1H), 6.98 (d, J = 7.8 Hz, 1H), 7.22 (t, J = 7.8 Hz, 1H), 7.26–7.38 (m, 2H), 7.45 (t, J = 8.9 Hz, 1H), 7.73–7.80 (m, 3H), 8.00 (t, J = 8.9 Hz, 1H), 8.06 (d, J = 8.9 Hz, 1H), 8.33 (d, J = 8.9 Hz, 1H), 8.98 ppm (s, 1H): ^{13}C NMR (300 MHz, $CDCl_3$ + 1 drop [D]TFA): δ = 165.5, 163.4, 142.1, 140.7, 136.7, 133.8, 132.33, 130.7, 128.2, 126.5, 124.8, 123.1, 122.1, 121.4, 119.4, 117.8, 117.2, 115.0, 114.2, 111.1 ppm; MS (ESI): 355 $[M+H]^+$; HRMS (ESI) calcd for $C_{22}H_{15}N_3OF$ $[M+H]^+$ 356.1194; found: 356.1201.

(*E*)-5-Fluoro-3-((2-(4-fluorophenyl)imidazo[1,2-*a*]pyridin-3-yl)methylene)indolin-2-one (10d): Compound **10d** was prepared according to the method described for compound **10a**, employing 2-(4-fluorophenyl)imidazo[1,2-*a*]pyridine-3-carbaldehyde **8b** (200 mg, 0.83 mmol) and 5-fluoroindolin-2-one **9b** (126 mg, 0.83 mmol) to obtain the pure product **10d** as a yellow solid (159 mg, 51%); mp: 291–292 °C; IR (KBr) $\tilde{\nu}$ = 3431, 3004, 1633, 772 cm^{-1}; ^{1}H NMR (300 MHz, $CDCl_3$): δ = 6.16 (dd, J = 2.0 Hz, J = 7.5 Hz, 1H), 7.02 (dd, J = 2.9, 7.5 Hz, 1H), 7.17 (dt, J = 2.0, 7.5 Hz, 1H), 7.26–7.31 (m, 2H), 7.45–7.48 (m, 1H), 7.69–7.75 (m, 2H), 7.82 (s, 1H), 8.00 (t, J = 8.4 Hz, 1H), 8.05 (d, J = 8.4 Hz, 1H), 8.18 (d, J = 8.4 Hz, 1H), 9.21 ppm (s, 1H); ^{13}C NMR (300 MHz, $CDCl_3$ + 1 drop [D]TFA): δ = 165.7, 163.7, 140.7, 140.1, 137.4, 137.1, 136.9, 134.6, 131.4, 130.5, 128.2, 126.3, 121.6, 118.4, 117.4, 117.3, 114.2, 113.1, 112.2 ppm; MS (ESI): 374 $[M+H]^+$; HRMS (ESI) calcd for $C_{22}H_{14}N_3OF_2$ $[M+H]^+$ 374.1105; found: 374.1112.

(*E*)-5-Chloro-3-((2-(4-fluorophenyl)imidazo[1,2-*a*]pyridin-3-yl)methylene)indolin-2-one (10e): Compound **10e** was prepared according to the method described for compound **10a**, employing 2-(4-fluorophenyl)imidazo[1,2-*a*]pyridine-3-carbaldehyde **8b** (200 mg, 0.83 mmol) and 5-chloroindolin-2-one **9c** (139 mg, 0.83 mmol) to obtain the pure product **10e** as a yellow solid (188 mg, 58%); mp: 299–300 °C; IR (KBr) $\tilde{\nu}$ = 3430, 3226, 1702, 751 cm^{-1}; ^{1}H NMR (300 MHz, $CDCl_3$): δ = 6.39 (s, 1H), 6.89 (d, J = 7.8 Hz, 1H), 7.18–7.23 (m, 1H), 7.53 (t, J = 8.2 Hz, 1H), 7.71–7.78 (m, 2H), 7.82 (s, 1H), 7.97–8.11 (m, 3H), 8.21 (d, J = 8.2 Hz, 1H), 8.33 (d, J = 8.2 Hz, 1H), 9.06 ppm (s, 1H); ^{13}C NMR (300 MHz, $CDCl_3$ + 1 drop [D]TFA): δ = 169.6, 165.7, 140.6, 139.8, 137.0, 134.8, 132.0,

131.3, 130.4, 128.9, 128.2, 126.4, 125.0, 121.6, 120.5, 118.6, 117.5, 117.3, 113.7, 112.2, 111.4 ppm; MS (ESI): 390 $[M+H]^+$; HRMS (ESI) calcd for $C_{22}H_{14}N_3OClF$ $[M+H]^+$ 390.08; found: 390.08.

(*E*)-6-Chloro-3-((2-(4-fluorophenyl)imidazo[1,2-*a*]pyridin-3-yl)methylene)indolin-2-one (10 f): Compound **10 f** was prepared according to the method described for compound **10 a**, employing 2-(4-fluorophenyl)imidazo[1,2-*a*]pyridine-3-carbaldehyde **8 b** (200 mg, 0.83 mmol) and 6-chloroindolin-2-one **9 d** (139 mg, 0.83 mmol) to obtain the pure product **10 f** as a yellow solid (204 mg, 63%); mp: 315–316 °C; IR (KBr) $\tilde{\nu}$ = 3428, 3079, 1712, 758 cm^{-1}; ^1H NMR (300 MHz, CDCl3): δ = 6.24 (d, J = 7.1 Hz, 1H), 6.71 (d, J = 7.1 Hz, 1H), 7.09–7.16 (m, 1H), 7.41 (t, J = 6.9 Hz, 1H), 7.64–7.70 (m, 3H), 7.89 (t, J = 8.7 Hz, 1H), 7.94 (d, J = 7.7 Hz, 2H), 8.12 (d, J = 6.9 Hz, 1H), 8.22 (d, J = 6.9 Hz, 1H), 8.92 ppm (s, 1H); ^{13}C NMR (300 MHz, $CDCl_3$ + 1 drop [D]TFA): δ = 169.4, 163.6, 142.8, 140.6, 138.5, 136.7, 134.4, 132.3, 130.5, 128.1, 126.4, 125.6, 123.4, 122.3, 121.6, 118.3, 117.2, 115.5, 114.0, 112.0 ppm; MS (ESI): 390 $[M+H]^+$; HRMS (ESI) calcd for $C_{22}H_{14}N_3OClF$ $[M+H]^+$ 390.08; found: 390.08.

(*E*)-3-((2-(4-Fluorophenyl)imidazo[1,2-*a*]pyridin-3-yl)methylene)-5-methoxyindolin-2-one (10 g): Compound **10 g** was prepared according to the method described for compound **10 a**, employing 2-(4-fluorophenyl)imidazo[1,2-*a*]pyridine-3-carbaldehyde **8 b** (200 mg, 0.83 mmol) and 5-methoxyindolin-2-one **9 e** (136 mg, 0.83 mmol) to obtain the pure product **10 g** as a yellow solid (154 mg, 48%); mp: 261–262 °C; IR (KBr) $\tilde{\nu}$ = 3457, 3053, 1709, 746 cm^{-1}; ^1H NMR (300 MHz, $CDCl_3$): δ = 3.48 (s, 3H, OCH_3), 5.94 (s, 1H), 6.86 (dd, J = 2.2, 7.2 Hz, 1H), 6.91 (d, J = 7.2 Hz, 1H), 7.52 (t, J = 7.6 Hz, 1H), 7.76–7.78 (m, 3H), 8.04 (t, J = 7.6 Hz, 1H), 8.14 (d, J = 7.6 Hz, 1H), 8.26–8.29 (m, 3H), 9.12 ppm (s, 1H); ^{13}C NMR (300 MHz, $CDCl_3$ + 1 drop [D]TFA): δ = 169.6, 163.6, 156.0, 140.5, 136.5, 135.4, 134.4, 133.8, 130.5, 126.7, 121.6, 120.1, 118.2, 117.4, 116.2, 115.7, 113.9, 111.5, 107.6, 55.6 ppm; MS (ESI): 386 $[M+H]^+$; HRMS (ESI) calcd for $C_{23}H_{17}N_3O_2F$ $[M+H]^+$ 386.13; found: 386.13.

(*E*)-3-((2-(4-Chlorophenyl)imidazo[1,2-*a*]pyridin-3-yl)methylene) indolin-2-one (10 h): Compound **10 h** was prepared according to the method described for compound **10 a**, employing 2-(4-chlorophenyl)imidazo[1,2-*a*]pyridine-3-carbaldehyde **8 c** (200 mg, 0.78 mmol) and indolin-2-one **9 a** (104 mg, 0.78 mmol) to obtain the pure product **10 h** as a yellow solid (188 mg, 65%); mp: 280–281 °C; IR (KBr) $\tilde{\nu}$ = 3430, 3133, 1701, 754 cm^{-1}; ^1H NMR (300 MHz, $CDCl_3$): δ = 6.37 (d, J = 7.9 Hz, 1H), 6.84 (t, J = 7.9 Hz, 1H), 7.01 (d, J = 7.9 Hz, 1H), 7.33 (t, J = 7.9 Hz, 1H), 7.46–7.51 (m, 3H), 7.70–7.77 (m, 3H), 8.03 (t, J = 8.9 Hz, 1H), 8.08 (d, J = 8.9 Hz, 1H), 8.32 (d, J = 8.9 Hz, 1H), 9.60 ppm (s, 1H); ^{13}C NMR (300 MHz, $CDCl_3$ + 1 drop [D]TFA): δ = 179.2, 147.6, 141.0, 139.8, 138.4, 136.9, 134.4, 133.7, 132.6, 131.2, 130.4, 129.5, 123.6, 122.4, 119.8, 118.2, 116.0, 113.9, 112.1, 111.5 ppm; MS (ESI): 372 $[M+H]^+$; HRMS (ESI) calcd for $C_{22}H_{15}N_3OCl$ $[M+H]^+$ 372.0898; found: 372.0914.

(*E*)-3-((2-(4-Chlorophenyl)imidazo[1,2-*a*]pyridin-3-yl)methylene)-5-fluoroindolin-2-one (10 i): Compound **10 i** was prepared according to the method described for compound **10 a**, employing 2-(4-chlorophenyl)imidazo[1,2-*a*]pyridine-3-carbaldehyde **8 c** (200 mg, 0.78 mmol) and 5-fluoroindolin-2-one **9 b** (118 mg, 0.78 mmol) to obtain the pure product **10 i** as a yellow solid (212 mg, 70%); mp: 298–299 °C; IR (KBr) $\tilde{\nu}$ = 3432, 3159, 1705, 757 cm^{-1}; ^1H NMR (300 MHz, $CDCl_3$): δ = 6.13 (dd, J = 1.9, 7.8 Hz, 1H), 7.01 (dd, J = 3.2, 7.8 Hz, 1H), 7.16 (dt, J = 1.9, 7.8 Hz, 1H), 7.46 (t, J = 8.7 Hz, 1H), 7.55 (d, J = 6.8 Hz, 2H), 7.63 (d, J = 6.8 Hz, 2H), 7.80 (s, 1H), 7.99 (t, J = 8.7 Hz, 1H), 8.05 (d, J = 8.7 Hz, 1H), 8.18 (d, J = 8.7 Hz, 1H), 9.12 ppm (s, 1H); ^{13}C NMR (300 MHz, $CDCl_3$ + 1 drop [D]TFA): δ = 179.2, 169.6, 158.0, 140.6, 138.7, 136.5, 135.0, 133.1, 131.1, 130.3, 130.1, 129.2, 126.6, 123.7, 118.9, 118.6, 117.2, 116.0, 113.8, 112.2, 109.1 ppm; MS (ESI): 390 $[M+H]^+$; HRMS (ESI) calcd for $C_{22}H_{14}N_3OClF$ $[M+H]^+$ 390.08; found: 390.08.

(*E*)-5-Chloro-3-((2-(4-chlorophenyl)imidazo[1,2-*a*]pyridin-3-yl)methylene)indolin-2-one (10 j): Compound **10 j** was prepared according to the method described for compound **10 a**, employing 2-(4-chlorophenyl)imidazo[1,2-*a*]pyridine-3-carbaldehyde **8 c** (200 mg, 0.78 mmol) and 5-chloroindolin-2-one **9 c** (130 mg, 0.78 mmol) to obtain the pure product **10 j** as a yellow solid (215 mg, 68%); mp: 305–306 °C; IR (KBr) $\tilde{\nu}$ = 3434, 3040, 1685, 756 cm^{-1}; ^1H NMR (300 MHz, $CDCl_3$): δ = 6.35 (s, 1H), 6.88 (d, J = 7.6 Hz, 1H), 6.96 (d, J = 7.6 Hz, 1H), 7.39–7.44 (m, 1H), 7.54 (d, J = 6.8 Hz, 2H), 7.79 (s, 1H), 7.91 (t, J = 8.8 Hz, 1H), 8.01 (d, J = 6.8 Hz, 2H), 8.18 (d, J = 8.8 Hz, 1H), 8.34 (d, J = 8.8 Hz, 1H), 8.97 ppm (s, 1H); ^{13}C NMR (300 MHz, $CDCl_3$ + 1 drop [D]TFA): δ = 168.8, 140.8, 140.1, 138.3, 136.7, 134.5, 132.8, 131.8, 130.1, 129.3, 128.3, 126.5, 124.8, 124.1, 121.5, 118.3, 116.9, 114.0, 112.9, 112.1 ppm; MS (ESI): 406 $[M+H]^+$; HRMS (ESI) calcd for $C_{22}H_{14}N_3OCl_2$ $[M+H]^+$ 406.05; found: 406.05.

(*E*)-6-Chloro-3-((2-(4-chlorophenyl)imidazo[1,2-*a*]pyridin-3-yl)methylene)indolin-2-one (10 k): Compound **10 k** was prepared according to the method described for compound **10 a**, employing 2-(4-chlorophenyl)imidazo[1,2-*a*]pyridine-3-carbaldehyde **8 c** (200 mg, 0.78 mmol) and 6-chloroindolin-2-one **9 d** (130 mg, 0.78 mmol) to obtain the pure product **10 k** as a yellow solid (190 mg, 60%); mp: 278–279 °C; IR (KBr) $\tilde{\nu}$ = 3413, 3050, 1705, 749 cm^{-1}; ^1H NMR (300 MHz, $CDCl_3$): δ = 6.25 (d, J = 7.8 Hz, 1H), 6.77 (d, J = 7.8 Hz, 1H), 6.97 (s, 1H),7.39 (t, J = 8.7 Hz, 1H), 7.49 (d, J = 7.8 Hz, 2H), 7.69–7.79 (m, 3H), 7.92 (t, J = 8.7 Hz, 1H), 7.98 (d, J = 8.7 Hz, 1H), 8.38 (d, J = 8.7 Hz, 1H), 9.76 ppm (s, 1H); ^{13}C NMR (300 MHz, $CDCl_3$ + 1 drop [D]TFA): δ = 169.4, 142.7, 140.6, 138.5, 136.7, 134.4, 132.3, 131.2, 130.2, 129.4, 128.0, 126.4, 125.7, 123.8, 123.5, 122.3, 118.3, 117.0, 114.0, 112.1 ppm; MS (ESI): 406 $[M+H]^+$; HRMS (ESI) calcd for $C_{22}H_{14}N_3OCl_2$ $[M+H]^+$ 406.05; found: 406.05.

(*E*)-3-((2-(4-Chlorophenyl)imidazo[1,2-*a*]pyridin-3-yl)methylene)-5-methoxyindolin-2-one (10 l): Compound **10 l** was prepared according to the method described for compound **10 a**, employing 2-(4-chlorophenyl)imidazo[1,2-*a*]pyridine-3-carbaldehyde **8 c** (200 mg, 0.78 mmol) and 5-methoxyindolin-2-one **9 e** (127 mg, 0.78 mmol) to obtain the pure product **10 l** as a yellow solid (147 mg, yield 47%); mp: 268–269 °C; IR (KBr) $\tilde{\nu}$ = 3214, 1710, 758 cm^{-1}; ^1H NMR (300 MHz, CDCl3): δ = 3.46 (s, 3H), 5.87 (s, 1H), 6.83–6.86 (m, 2H), 7.43 (t, J = 8.9 Hz, 1H), 7.50 (d, J = 6.9 Hz, 2H), 7.61 (d, J = 6.9 Hz, 2H), 7.72 (s, 1H), 7.92–7.97 (m, 1H), 8.05 (d, J = 8.9 Hz, 1H), 8.27 (d, J = 8.9 Hz, 1H), 8.55 ppm (s, 1H); ^{13}C NMR (300 MHz, $CDCl_3$ + 1 drop [D]TFA): δ = 179.2, 156.1, 147.6, 140.5, 139.8, 136.8, 134.5, 131.2, 130.4, 130.2, 129.4, 126.7, 122.4, 119.8, 118.3, 117.6, 114.0, 113.8, 111.5, 55.6 ppm; MS (ESI): 402 $[M+H]^+$; HRMS (ESI) calcd for $C_{23}H_{17}N_3O_2Cl$ $[M+H]^+$ 402.10; found: 402.10.

(*E*)-3-((2-*para*-Tolylimidazo[1,2-*a*]pyridin-3-yl)methylene)indolin-2-one (10 m): Compound **10 m** was prepared according to the method described for compound **10 a**, employing 2-*p*-tolylimidazo-[1,2-*a*]pyridine-3-carbaldehyde **8 d** (200 mg, 0.85 mmol) and indolin-2-one **9 a** (113 mg, 0.85 mmol) to obtain the pure product **10 m** as a yellow solid (205 mg, 69%); mp: 263–264 °C; IR (KBr) $\tilde{\nu}$ = 3428, 3061, 1686, 746 cm^{-1}; ^1H NMR (300 MHz, $CDCl_3$): δ = 2.40 (s, 3H), 6.33 (d, J = 7.0 Hz, 1H), 6.83 (t, J = 8.9 Hz, 1H), 6.99 (d, J = 7.0 Hz, 1H), 7.29–7.32 (m, 3H), 7.42 (t, J = 8.0 Hz, 1H), 7.67 (d, J = 8.0 Hz, 2H), 7.75 (s, 1H), 7.97 (t, J = 8.0 Hz, 1H), 8.01 (d, J = 8.0 Hz, 1H), 8.36 (d, J = 8.0 Hz, 1H), 8.93 ppm (s, 1H); ^{13}C NMR (300 MHz, $CDCl_3$ + 1 drop [D]TFA): δ = 168.6, 142.3, 141.9, 140.8, 138.6, 133.1, 132.7,

132.0, 130.4, 129.2, 128.4, 126.3, 125.1, 123.0, 121.1, 119.7, 117.4, 114.6, 113.4, 110.9, 21.5 ppm; MS (ESI): 352 $[M+H]^+$; HRMS (ESI) calcd for $C_{23}H_{18}N_3O$ $[M+H]^+$ 352.14; found: 352.14.

(*E*)-5-Fluoro-3-((2-*para*-tolylimidazo[1,2-*a*]pyridin-3-yl)methylene)indolin-2-one (10n): Compound **10n** was prepared according to the method described for compound **10a**, employing 2-*p*-tolylimidazo[1,2-*a*]pyridine-3-carbaldehyde **8d** (200 mg, 0.85 mmol) and 5-fluoroindolin-2-one **9b** (128 mg, 0.85 mmol) to obtain the pure product **10n** as a yellow solid (221 mg, 71%); mp: 305–306 °C; IR (KBr) $\tilde{\nu}=3389$, 2934, 1627, 803 cm^{-1}; ^1H NMR (300 MHz, $CDCl_3$): $\delta=2.45$ (s, 3H), 6.12 (dd, $J=2.9$ Hz, $J=7.8$ Hz, 1H), 6.99 (d, $J=7.8$ Hz, 1H), 7.14 (dt, $J=2.9$, 7.8 Hz, 1H), 7.38 (d, $J=7.4$ Hz, 2H), 7.49 (t, $J=8.7$ Hz, 1H), 7.57 (d, $J=7.4$ Hz, 2H), 7.83 (s, 1H), 7.95 (t, $J=8.7$ Hz, 1H), 8.00 (d, $J=8.7$ Hz, 1H), 8.19 (d, $J=8.7$ Hz, 1H), 9.11 ppm (s, 1H); ^{13}C NMR (300 MHz, $CDCl_3$ + 1 drop [D]TFA): $\delta=$ 169.6, 157.8, 143.0, 140.6, 138.2, 136.7, 134.3, 132.2, 130.6, 129.0, 128.1, 126.4, 122.5, 118.2, 117.2, 115.4, 114.0, 112.5, 111.9, 108.7, 21.4 ppm; MS (ESI): 370 $[M+H]^+$; HRMS (ESI) calcd for $C_{23}H_{17}N_3OF$ $[M+H]^+$ 370.14; found: 370.13.

(*E*)-5-Chloro-3-((2-*para*-tolylimidazo[1,2-*a*]pyridin-3-yl)methylene)indolin-2-one (10o): Compound **10o** was prepared according to the method described for compound **10a**, employing 2-*p*-tolylimidazo[1,2-*a*]pyridine-3-carbaldehyde **8d** (200 mg, 0.85 mmol) and 5-chloroindolin-2-one **9c** (141 mg, 0.85 mmol) to obtain the pure product **10o** as a yellow solid (209 mg, 64%); mp: 264–265 °C; IR (KBr) $\tilde{\nu}=3441$, 3052, 1707, 751 cm^{-1}; ^1H NMR (300 MHz, $CDCl_3$): $\delta=2.44$ (s, 3H), 6.32 (s, 1H), 6.98 (d, $J=6.0$ Hz, 1H), 7.30 (d, $J=6.0$ Hz, 1H), 7.36–7.43 (m, 3H), 7.56 (d, $J=8.0$ Hz, 2H), 7.82 (s, 1H), 7.93 (t, $J=9.1$ Hz, 1H), 7.98 (d, $J=9.1$ Hz, 1H), 8.18 (d, $J=$ 9.1 Hz, 1H), 9.12 ppm (s, 1H); ^{13}C NMR (300 MHz, $CDCl_3$ + 1 drop [D]TFA): $\delta=166.4$, 142.6, 140.7, 140.1, 138.4, 133.8, 131.4, 130.5, 128.1, 128.1, 126.4, 125.0, 122.8, 121.2, 117.9, 115.6, 114.1, 112.9, 111.8, 21.4 ppm; MS (ESI): 386 $[M+H]^+$; HRMS (ESI) calcd for $C_{23}H_{17}N_3OCl$ $[M+H]^+$ 386.13; found: 386.13.

(*E*)-6-Chloro-3-((2-*para*-tolylimidazo[1,2-*a*]pyridin-3-yl)methylene)indolin-2-one (10p): Compound **10p** was prepared according to the method described for compound **10a**, employing 2-*p*-tolylimidazo[1,2-*a*]pyridine-3-carbaldehyde **8d** (200 mg, 0.85 mmol) and 6-chloroindolin-2-one **9d** (141 mg, 0.85 mmol) to obtain the pure product **10p** as a yellow solid (189 mg, 58%); mp: 283–284 °C; IR (KBr) $\tilde{\nu}=3429$, 3042, 1687, 755 cm^{-1}; ^1H NMR (300 MHz, $CDCl_3$): $\delta=2.41$ (s, 3H), 6.31 (d, $J=8.1$ Hz, 1H), 6.82 (dd, $J=1.8$, 8.1 Hz, 1H), 7.06 (s, 1H), 7.34 (d, $J=7.9$ Hz, 2H), 7.50–7.59 (m, 3H), 7.80 (s, 1H), 8.02–8.11 (m, 2H), 8.24 (d, $J=8.8$ Hz, 1H), 9.41 ppm (s, 1H); ^{13}C NMR (300 MHz, $CDCl_3$ + 1 drop [D]TFA): $\delta=143.1$, 140.3, 138.2, 137.8, 134.4, 130.6, 130.5, 128.8, 128.0, 126.5, 125.7, 123.4, 122.2, 118.3, 115.6, 113.6, 112.0, 21.4 ppm: MS (ESI): 386 $[M+H]^+$; HRMS (ESI) calcd for $C_{23}H_{17}N_3OCl$ $[M+H]^+$ 386.11; found: 386.11.

(*E*)-5-Methoxy-3-((2-*para*-tolylimidazo[1,2-*a*]pyridin-3-yl)methylene)indolin-2-one (10q): Compound **10q** was prepared according to the method described for compound **10a**, employing 2-*p*-tolylimidazo[1,2-*a*]pyridine-3-carbaldehyde **8d** (200 mg, 0.85 mmol) and 5-methoxyindolin-2-one **9e** (138 mg, 0.85 mmol) to obtain the pure product **10q** as a yellow solid (139 mg, 43%); mp: 250–251 °C; IR (KBr) $\tilde{\nu}=3395$, 2927, 1627, 808 cm^{-1}; ^1H NMR (300 MHz, $CDCl_3$): $\delta=2.41$ (s, 3H), 3.47 (s, 3H), 5.93 (s, 1H), 6.85 (dd, $J=2.2$, 8.4 Hz, 1H), 6.94 (d, $J=8.4$ Hz, 1H), 7.35 (d, $J=7.9$ Hz, 2H), 7.52 (t, $J=6.9$ Hz, 1H), 7.62 (d, $J=7.9$ Hz, 2H), 7.79 (s, 1H), 8.04 (t, $J=$ 6.9 Hz, 1H), 8.11 (d, $J=6.9$ Hz, 1H), 8.28 (d, $J=6.9$ Hz, 1H), 9.32 ppm (s, 1H); ^{13}C NMR (300 MHz, $CDCl_3$ + 1 drop [D]TFA): $\delta=$ 169.8, 156.1, 143.0, 140.3, 137.6, 135.2, 134.3, 133.4, 130.6, 128.1, 126.8, 122.3, 120.2, 118.2, 117.5, 115.7, 113.6, 113.2, 111.4, 109.4, 55.6, 21.4 ppm; MS (ESI): 381 $[M+H]^+$.

(*E*)-5-Fluoro-3-((2-(4-methoxyphenyl)imidazo[1,2-*a*]pyridin-3-yl)methylene)indolin-2-one (10r): Compound **10r** was prepared according to the method described for compound **10a**, employing 2-(4-methoxyphenyl)imidazo[1,2-*a*]pyridine-3-carbaldehyde **8e** (200 mg, 0.79 mmol) and 5-fluoroindolin-2-one **9b** (120 mg, 0.79 mmol) to obtain the pure product **10r** as a yellow solid (171 mg, 56%); mp: 251–252 °C; IR (KBr) $\tilde{\nu}=3080$, 1707, 744 cm^{-1}; ^1H NMR (300 MHz, $CDCl_3$): $\delta=3.86$ (s, 3H), 6.14 (dd, $J=2.2$, 7.1 Hz, 1H), 6.96–7.05 (m, 2H), 7.46–7.55 (m, 3H), 7.67 (d, $J=8.4$ Hz, 2H), 7.85 (s, 1H), 8.04 (t, $J=8.1$ Hz, 1H), 8.14 (d, $J=8.1$ Hz, 1H), 8.24 (d, $J=8.12$ Hz, 1H), 9.36 ppm (s, 1H); ^{13}C NMR (300 MHz, $CDCl_3$ + 1 drop [D]TFA): $\delta=170.2$, 162.7, 140.4, 138.2, 134.4, 131.7, 130.8, 129.9, 128.4, 126.4, 120.4, 118.3, 117.6, 117.2, 115.5, 114.8, 113.8, 112.7, 112.0, 108.8, 55.5 ppm; MS (ESI): 386 $[M+H]^+$; HRMS (ESI) calcd for $C_{23}H_{17}N_3O_2F$ $[M+H]^+$ 386.13; found: 386.13.

(*E*)-5-Chloro-3-((2-(4-methoxyphenyl)imidazo[1,2-*a*]pyridin-3-yl)methylene)indolin-2-one (10s): Compound **10s** was prepared according to the method described for compound **10a**, employing 2-(4-methoxyphenyl)imidazo[1,2-*a*]pyridine-3-carbaldehyde **8e** (200 mg, 0.79 mmol) and 5-chloroindolin-2-one **9c** (132 mg, 0.79 mmol) to obtain the pure product **10d** as a yellow solid (159 mg, 50%); mp: 257–258 °C; IR (KBr) $\tilde{\nu}=3376$, 3065, 1757, 840 cm^{-1}; ^1H NMR (300 MHz, $CDCl_3$): $\delta=3.86$ (s, 3H), 6.40 (s, 1H), 6.94–7.03 (m, 2H), 7.24–7.28 (m, 2H), 7.53–7.64 (m, 3H), 7.88 (s, 1H), 8.08 (t, $J=8.3$ Hz, 1H), 8.18–8.25 (m, 2H), 9.39 ppm (s, 1H); ^{13}C NMR (300 MHz, $CDCl_3$ + 1 drop [D]TFA): $\delta=162.7$, 140.3, 139.9, 138.7, 138.0, 134.8, 131.7, 130.7, 129.7, 128.5, 126.5, 125.3, 121.5, 118.5, 117.8, 115.6, 113.5, 113.0, 112.6, 109.2, 55.5 ppm; MS (ESI): 402 $[M+H]^+$; HRMS (ESI) calcd for $C_{23}H_{17}N_3O_2Cl$ $[M+H]^+$ 402.10; found: 402.10.

(*E*)-6-Chloro-3-((2-(4-methoxyphenyl)imidazo[1,2-*a*]pyridin-3-yl)methylene)indolin-2-one (10t): Compound **10t** was prepared according to the method described for compound **10a**, employing 2-(4-methoxyphenyl)imidazo[1,2-*a*]pyridine-3-carbaldehyde **8e** (200 mg, 0.79 mmol) and 6-chloroindolin-2-one **9d** (132 mg, 0.79 mmol) to obtain the pure product **10t** as a yellow solid (187 mg, 59%); mp: 221–222 °C; IR (KBr) $\tilde{\nu}=3463$, 3079, 1713, 760 cm^{-1}; ^1H NMR (300 MHz, $CDCl_3$): $\delta=3.89$ (s, 3H), 6.33 (d, $J=$ 8.3 Hz, 1H), 6.82 (dd, $J=1.3$, 8.3 Hz, 1H), 7.10 (s, 1H), 7.19 (d, $J=$ 8.1, 2H), 7.55–7.67 (m, 3H), 7.78 (s, 1H), 7.94–8.05 (m, 2H), 8.12 (d, $J=7.9$ Hz, 1H), 9.3 ppm (s, 1H); ^{13}C NMR (300 MHz, $CDCl_3$ + 1 drop [D]TFA): $\delta=162.6$, 140.9, 139.8, 138.4, 137.2, 134.4, 130.7, 129.8, 128.3, 125.8, 123.9, 122.2, 120.5, 118.3, 117.4, 115.4, 113.6, 112.6, 112.0, 109.1, 55.5 ppm; MS (ESI): 402 $[M+H]^+$; HRMS (ESI) calcd for $C_{23}H_{17}N_3O_2Cl$ $[M+H]^+$ 402.10; found: 402.10.

Acknowledgements

V.S.R, A.B.S, G.B.K., M.P.N.R., and C.K. acknowledge the Council of Scientific & Industrial Research (CSIR)–University Grant Commission (UGC), New Delhi (India) for the award of senior research fellowships. The authors also acknowledge the CSIR for financial support under the 12th Five-Year Plan projects "Affordable Cancer Therapeutics (ACT)" (CSC0301) and "Small Molecules in Lead Exploration (SMiLE)" (CSC0111). Finally, the authors thank Dr. K. Ravinder and Dr. Rakesh K. Mishra (Centre for Cellular & Molecular Biology, Hyderabad, India) for assistance with zebra fish assays.

Keywords: apoptosis · cytotoxicity · imidazopyridine–oxindoles · molecular docking · tubulin polymerisation

[1] M. Garcia, A. Jemal, E. M. Ward, M. M. Center, Y. Hao, R. L. Siegel, M. J. Thun, *Global Cancer Facts & Figures*, 2nd ed., American Cancer Society, Atlanta, USA, **2007**: http://www.cancer.org/acs/groups/content/@nho/documents/document/globalfactsandfigures2007rev2p.pdf (accessed August 28, 2013).
[2] a) F. Pellegrini, D. R. Budman, *Cancer Invest.* **2005**, *23*, 264 – 273; b) S. Honore, E. Pasquier, D. Braguer, *Cell. Mol. Life Sci.* **2005**, *62*, 3039 – 3065.
[3] M. A. Jordan, L. Wilson, *Nat. Rev. Cancer* **2004**, *4*, 253 – 265.
[4] a) J. Löwe, H. Li, K. Downing, E. Nogales, *J. Mol. Biol.* **2001**, *313*, 1045 – 1057; b) B. Gigant, C. Wang, R. B. G. Ravelli, F. Roussi, M. O. Steinmetz, P. A. Curmi, A. Sobel, M. Knossow, *Nature* **2005**, *435*, 519 – 522.
[5] Z. Chen, P. J. Merta, N. H. Lin, S. K. Tahir, P. Kovar, H. L. Sham, H. Zhang, *Mol. Cancer Ther.* **2005**, *4*, 562 – 568.
[6] A. Jordan, J. A. Hadfield, N. J. Lawrence, A. T. McGown, *Med. Res. Rev.* **1998**, *18*, 259 – 296.
[7] H. Zhuang, W. Jiang, W. Cheng, K. Qian, W. Dong, L. Cao, Q. Huang, S. Li, J. F. Chiu, X. X. Fang, M. Lu, Z. C. Hua, *Lung Cancer* **2009**.
[8] F. D. Boyer, J. Dubois, S. Thoret, M. E. T. H. Dau, I. Hanna, *Bioorg. Chem.* **2010**, *38*, 149 – 158.
[9] M. N. Semenova, A. S. Kiselyov, D. V. Tsyganov, L. D. Konyushkin, S. I. Firgang, R. V. Semenov, O. R. Malyshev, M. M. Raihstat, F. Fuchs, A. Stielow, M. Lantow, A. A. Philchenkov, M. P. Zavelevich, N. S. Zefirov, S. A. Kuznetsov, V. V. Semenov, *J. Med. Chem.* **2011**, *54*, 7138 – 7149.
[10] B. L. Flynn, G. S. Gill, D. W. Grobelny, J. H. Chaplin, D. Paul, A. F. Leske, T. C. Lavranos, D. K. Chalmers, S. A. Charman, E. Kostewicz, D. M. Shackleford, J. Morizzi, E. Hamel, M. K. Jung, G. Kremmidiotis, *J. Med. Chem.* **2011**, *54*, 6014 – 6027.
[11] G. R. Pettit, G. M. Cragg, D. L. Herald, J. M. Schmidt, P. Lohavanijaya, *Can. J. Chem.* **1982**, *60*, 1374 – 1376.
[12] H. Hsieh, J. Liou, N. Mahindroo, *Curr. Pharm. Des.* **2005**, *11*, 1655 – 1677.
[13] N. H. Nam, *Curr. Med. Chem.* **2003**, *10*, 1697 – 1722.
[14] J. J. Cui, M. McTigue, M. Nambu, M. Tran-Dubé, M. Pairish, H. Shen, L. Jia, H. Cheng, J. Hoffman, P. Le, M. Jalaie, G. H. Goetz, K. Ryan, N. Grodsky, Y. L. Deng, M. Parker, S. Timofeevski, B. W. S. M. Yamazaki, S. Aguirre, Q. Li, H. Zou, J. Christensen, *J. Med. Chem.* **2012**, *55*, 8091 – 8109.
[15] P. Singh, M. Kaur, S. Sachdeva, *J. Med. Chem.* **2012**, *55*, 6381 – 6390.
[16] A. Kamal, G. Ramakrishna, P. Raju, A. V. S. Rao, A. Viswanath, V. L. Nayak, S. Ramakrishna, *Eur. J. Med. Chem.* **2011**, *46*, 2427 – 2435; b) A. Kamal, M. K. Reddy, T. B. Shaik, Y. V. V. Srikanth, V. S. Reddy, G. B. Kumar, S. V. Kalivendi, *Eur. J. Med. Chem.* **2012**, *50*, 9 – 17; c) A. Kamal, Y. V. V. Srikanth, T. B. Shaik, M. N. A. Khan, M. Ashraf, M. K. Reddy, K. A. Kumar, S. V. Kalivendi, *Med. Chem. Commun.* **2011**, *2*, 819 – 823.
[17] H. N. Bramson, J. Corona, S. T. Davis, S. H. Dickerson, M. Edelstein, S. V. Frye, R. T. Gampe, Jr., P. A. Harris, A. Hassell, W. D. Holmes, R. N. Hunter, K. E. Lackey, B. Lovejoy, M. J. Luzzio, V. Montana, W. J. Rocque, D. Rusnak, L. Shewchuk, J. M. Veal, D. H. Walker, L. F. Kuyper, *J. Med. Chem.* **2001**, *44*, 4339 – 4358.
[18] H. Mikashima, K. Goto, *Yakugaku Zasshi* **1982**, *102*, 99 – 103.
[19] J. I. Raats, G. Falkson, H. C. Falkson, *J. Clin. Oncol.* **1992**, *10*, 111 – 116.
[20] P. Singh, M. Kaur, W. Holzer, *Eur. J. Med. Chem.* **2010**, *45*, 4968 – 4982.
[21] A. Kamal, Y. V. Srikanth, M. N. Khan, T. B. Shaik, M. Ashraf, *Bioorg. Med. Chem. Lett.* **2010**, *20*, 5229 – 5231.
[22] a) A. Andreani, A. Locatelli, A. Leoni, M. Rambaldi, R. Morigi, R. Bossa, M. Chiericozzi, A. Fraccari, I. Galatulas, *Eur. J. Med. Chem.* **1997**, *32*, 919 – 924; b) A. Andreani, S. Burnelli, M. Granaiola, A. Leoni, A. Locatelli, R. Morigi, M. Rambaldi, L. Varoli, N. Calonghi, C. Cappadone, M. Voltattorni, M. Zini, C. Stefanelli, L. Masotti, R. H. Shoemaker, *J. Med. Chem.* **2008**, *51*, 7508 – 7513; c) A. Andreani, S. Burnelli, M. Granaiola, A. Leoni, A. Locatelli, R. Morigi, M. Rambaldi, L. Varoli, N. Calonghi, C. Cappadone, G. Farruggia, M. Zini, C. Stefanelli, L. Masotti, *J. Med. Chem.* **2007**, *50*, 3167 – 3172.
[23] A. Andreani, M. Granaiola, A. Leoni, A. Locatelli, R. Morigi, M. Rambaldi, G. Giorgi, L. Salvini, V. Garaliene, *Anti-Cancer Drug Des.* **2001**, *16*, 167 – 174.
[24] A. Kamal, J. S. Reddy, M. J. Ramaiah, D. Dastagiri, E. V. Bharathi, M. V. P. Sagar, S. N. C. V. L. Pushpavalli, P. Ray, M. P. Bhadra, *Med. Chem. Commun.* **2010**, *1*, 355 – 360.
[25] A. Dhanasekaran, S. Kotamraju, S. V. Kalivendi, T. Matsunaga, T. Shang, A. Keszler, J. Joseph, B. Kalyanaraman, *J. Biol. Chem.* **2004**, *279*, 37575 – 37587.
[26] Y. Zhang, X. Wang, W. Fang, X. Cai, F. Chu, X. Liao, J. Lu, *Bioinorg. Chem. Appl.* **2013**, 437134.
[27] L. I. Zon, R. T. Peterson, *Nat. Rev. Drug Discovery* **2005**, *4*, 35 – 44.
[28] H. S. Moon, E. M. Jacobson, S. M. Khersonsky, M. R. Luzung, D. P. Walsh, W. Xiong, J. W. Lee, P. B. Parikh, J. C. Lam, T. W. Kang, G. R. Rosania, A. F. Schier, Y. T. Chang, *J. Am. Chem. Soc.* **2002**, *124*, 11608 – 11609.
[29] C. B. Kimmel, W. W. Ballard, S. R. Kimmel, B. Ullmann, T. F. Schilling, *Dev. Dyn.* **1995**, *203*, 253 – 310.
[30] AutoDock version 4.2: http://autodock.scripps.edu/ (accessed August 28, 2013).
[31] R. B. Ravelli, B. Gigant, P. A. Curmi, I. Jourdain, S. Lachkar, A. Sobel, M. Knossow, *Nature* **2004**, *428*, 198 – 202.
[32] S. Kotamraju, C. L. Williams, B. Kalyanaraman, *Cancer Res.* **2007**, *67*, 7386 – 7394.
[33] D. Bonne, C. Heuséle, C. Simon, D. Pantaloni, *J. Biol. Chem.* **1985**, *260*, 2819 – 2825.
[34] K. Huber, P. Patel, I. Zhang, H. Evans, A. D. Westwell, P. M. Fischer, S. Chan, S. Martin, *Mol. Cancer Ther.* **2008**, *7*, 143 – 151.
[35] S. Kotamraju, Y. Tampo, A. Keszler, C. R. Chitambar, J. Joseph, A. L. Haas, B. Kalyanaraman, *Proc. Natl. Acad. Sci. USA* **2003**, *100*, 10653 – 10658.
[36] G. M. Morris, D. S. Goodsell, R. S. Halliday, R. Huey, W. E. Hart, R. K. Belew, A. J. Olson, *J. Comput. Chem.* **1998**, *19*, 1639 – 1662.

Received: July 12, 2013
Published online on September 23, 2013